

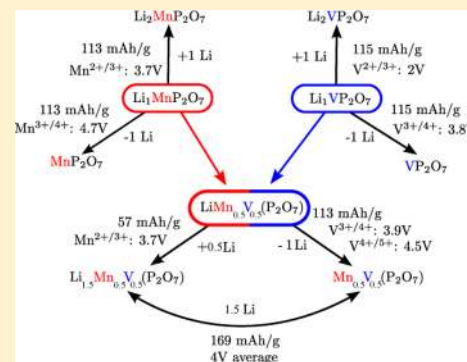
Designing Multielectron Lithium-Ion Phosphate Cathodes by Mixing Transition Metals

Geoffroy Hautier,[†] Anubhav Jain,[‡] Tim Mueller,[§] Charles Moore, Shyue Ping Ong, and Gerbrand Ceder*

Department of Materials Science and Engineering, Massachusetts Institute of Technology, 77 Massachusetts Avenue, Cambridge, Massachusetts 02139, United States

ABSTRACT: Finding new polyanionic Li-ion battery cathodes with higher capacities than LiFePO₄ is currently a major target of battery research. One approach toward this goal is to develop materials capable of exchanging more than one Li atom per transition metal. However, constraints on operating voltage due to organic electrolyte stability as well as cathode structural stability have made this target difficult to reach. More specifically, it is very challenging to develop a phosphate-based cathode in which a single element provides +2 to +4 redox activity in a reasonable voltage window: Either the voltage for the +2/+3 couple is too low (e.g., V) or the voltage for the +3/+4 couple is too high (e.g., Fe). This makes several appealing structural frameworks such as tavorite difficult to use as practical two-electron systems. Here, we propose a voltage design strategy based on the mixing of different transition metals in crystal structures known to be able to accommodate lithium in insertion and delithiation. By mixing a metal active on the +2/+3 couple (e.g., Fe) with an element active on the +3/+5 or +3/+6 couples (e.g., V or Mo), we show that high-capacity multielectron cathodes can be designed in an adequate voltage window. We illustrate our mixing strategy on LiMP₂O₇ pyrophosphates as well as LiMPO₄(OH) and LiM(PO₄)F tavorites, and we use density functional theory (DFT) computations to evaluate the theoretical capacity, voltage profile, and stability of the compounds proposed by our design rules. From this analysis, we identify several new compounds of potential interest as cathode materials.

KEYWORDS: Li-ion battery, cathode, phosphates, *ab initio*, DFT, tavorite, pyrophosphate, multielectron cathode



1. INTRODUCTION

Strong research efforts are currently focused on finding new Li-ion battery cathode materials with high energy density, low cost, and high safety.^{1–3} Because of the high thermal stability and rate capability of the iron phosphate olivine LiFePO₄,⁴ phosphate-based cathode materials have been attracting much attention from the battery community. However, current phosphate electrode materials face limitations, in terms of specific energy and energy density, and a phosphate-based cathode with high energy density is greatly sought.

The energy density of a cathode is the product of two parameters: voltage and capacity. Therefore, searching for materials with higher voltage but capacity similar to that of iron phosphate is one strategy to improve energy density. This is, for instance, the reason for the strong interest in LiMnPO₄ which provides a higher voltage at a similar capacity as LiFePO₄ but unfortunately shows poorer rate performance.^{5–8} However, generally speaking, increasing the voltage can lead to issues in terms of electrolyte decomposition (commercial electrolytes are only stable up to ~4.5 V), and higher voltage materials generally have lower intrinsic thermal stability in the charged state, which causes safety concerns.^{9,10} The alternative strategy is to find phosphate materials with higher capacities. Unfortunately, the capacity of phosphate materials exchanging one Li atom per transition metal during the electrochemical process is intrinsically limited, and olivine LiFePO₄ is already

among the one-electron phosphate cathodes with the highest volumetric and gravimetric capacities.¹⁰

The remaining option for increasing the capacity of phosphate-based cathodes is to use multielectron systems (i.e., materials that could cycle more than one Li atom per active transition metal). As we recently showed,¹⁰ the choice of practical multielectron redox couples is limited in phosphates. For the most common +2/+4 two-electron redox couple in phosphates, either the +3/+4 voltage is too high for current electrolytes (e.g., Fe, Mn, Co, ...) or the +2/+3 couple is too low in voltage (e.g., V and Mo). This voltage issue excludes from practical use many interesting phosphate-based structures that could be used on a +2/+4 couple.

It has been demonstrated experimentally that by mixing transition metals different redox couples can be activated in insertion or delithiation (see, e.g., the studies from Goodenough et al. on LiFe_{0.5}Mn_{0.5}PO₄⁴ and Li₃FeV(PO₄)₂¹¹).

In this paper, we present a strategy to design multielectron materials active in the voltage stability window of commercial electrolyte by mixing two transition metals in a crystal structure possessing adequate sites for activating a +2/+4 couple. By mixing one transition metal with a +2/+3 couple active in a

Received: January 17, 2013

Revised: April 22, 2013

voltage window of 2–4.5 V (e.g., Co, Fe, Mn or Cr) with V or Mo (which can be activated up to +5 or +6 for a voltage of <4.5 V), compounds can be formed with the potential to activate the +2/+3 couple of the first element as well as the +3/+5 or +3/+6 couples of the second element. Therefore, more than one Li atom per transition metal could be theoretically exchanged, leading to higher theoretical capacities. After describing, in detail, the mixing strategy and its application to a few phosphate-based structures, we use state-of-the-art ab initio computations^{12,13} to compute the stability and voltage of those designed compounds as well as their theoretical specific energies, energy densities, and thermal stability in the charged state. From this analysis, we suggest and discuss a few novel mixed compounds with potentially higher energy density than LiFePO_4 and with attractive voltages.

2. METHODS

All ab initio computations were performed in the density functional theory (DFT) framework using a generalized gradient approximation (GGA) functional parametrized by Perdew-Burke and Ernzerhof (PBE).¹⁴ The transition metals, Fe, Cr, Co, Mn, V, and Mo, have been assigned a U parameter to correct for the self-interaction error present in GGA.^{15,16} This U parameter was fitted to experimental binary oxides formation energies from the Kubaschewski tables, following the approach of Wang et al.^{17,18} For cobalt, a value of $U = 5.7$ eV was used. All compounds were initialized in their ferromagnetic states with a k -point density of at least 500/(number of atom in unit cell) k -points. Our previous work on fluoro-tavorite¹⁹ and antiferromagnetic computations on $\text{Li}_x\text{MPO}_4(\text{OH})$ and $\text{Li}_x\text{MP}_2\text{O}_7$ (with $x = 0, 1, 2$ and $M = \text{Mn, Fe, Co, V, Mo, Cr}$) showed that the difference in energy between the antiferromagnetic and ferromagnetic configuration was small (<7 meV/atom). The Vienna ab initio software package (VASP) was used with plane-augmented wave (PAW) pseudo-potentials.^{20,21} The computations are expected to be converged within a few meV/atom.²² All VASP computations were run using the AFLOW²³ code and more details on the high-throughput ab initio methodology and parameters can be found in Jain et al.²²

Thermodynamic stability was evaluated using ab initio computed total energies. The stability of any phase was evaluated by comparing it to other phases or linear combination of phases leading to the same composition using the *convex hull* construction.²⁴ The stability analysis was performed versus all compounds present in the Inorganic Crystal Structure Database (ICSD) database plus a set of phosphates predicted in our previous work.¹⁰ GGA and GGA+ U computations were combined using Jain et al.'s methodology.²⁵ The stability of any compound was quantified by evaluating the *energy above the hull*, which represents the magnitude of a compound's decomposition energy. An energy above the hull is always positive and measures the thermodynamic driving force for the compound to decompose into a set of alternative phases. A thermodynamically stable compound will have an energy above the hull of 0 meV/atom, because it is part of the convex hull of stable phases.

The voltage versus a lithium metal anode associated with the extraction of lithium from the material was computed using the methodology presented in Aydinol et al.²⁶ The entropic contribution to the voltage was neglected.

When the exact ordering of lithium (i.e., for partial delithiations) was unknown, we used an enumeration ordering algorithm similar to that developed by Hart et al. and chose the ordering associated with the lowest electrostatic energy computed by an Ewald sum.²⁷

Potential lithium insertion sites were identified using a dense grid search of the potential energy surface generated by an electrostatic potential model. This potential model was derived from the valence method and is similar to that recently developed by Adams and Rao.²⁸

Safety or thermal stability was computed as in Ong et al. by evaluating the oxygen chemical potential necessary for the compound to decompose at equilibrium through oxygen gas evolution.²⁹ This

approach assumes an equilibrium process and an entropic contribution to the reaction solely from the oxygen gas. The oxygen chemical potential reference ($\mu_{\text{O}_2} = 0$ meV) is chosen to be air at 298 K, according to the tabulated entropy of oxygen in the JANAF tables and the fitted oxygen molecule energy from Wang et al.^{17,30} Oxygen chemical potential ranges (with respect to this reference) can be found for typical binary oxides in the supporting information of the paper written by Hautier et al.³¹

3. RESULTS

3.1. Limits of Single Transition-Metal Phosphates in Terms of Two-Electron Couples.

Figure 1 shows the

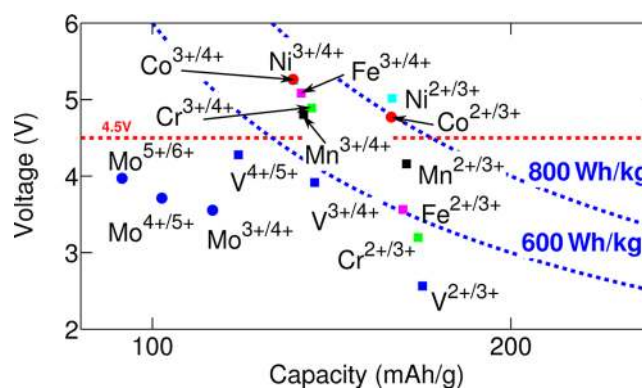


Figure 1. Average voltage versus capacity for different redox couples in phosphates. The voltages have been obtained computationally through high-throughput GGA+ U computations, while the capacity corresponds to the maximal capacity achievable. The data are reproduced from Hautier et al.¹⁰

computed average voltage expected from delithiation of a relatively stable compound versus the maximum gravimetric capacity achievable in phosphates for one-electron cathodes.¹⁰ Each data point corresponds to a redox couple, and a limit for commercial electrolyte stability of ~ 4.5 V is indicated as a dashed red line. Dashed blue lines of iso-specific energy are also drawn. The most common phosphate cathode material, olivine LiFePO_4 , has a specific energy of ~ 600 Wh/kg.

From Figure 1, we observe that it will be difficult to beat the gravimetric capacity of LiFePO_4 (i.e., 170 mAh/g) with a one-electron phosphate cathode. Increasing the specific energy can be achieved by using electrodes with similar capacity and higher voltage than LiFePO_4 but keeping the voltage in a reasonable range. The $\text{Mn}^{2+}/\text{Mn}^{3+}$ couple is an ideal target for this purpose, but LiMnPO_4 has not yet demonstrated good enough electrochemical performances to enable commercialization.^{5–8} Other olivine-based materials such as LiNiPO_4 and LiCoPO_4 show voltages significantly higher than 4.5 V, but are likely to be limited by the stability of the electrode and the high oxidation strength of the charged cathodes. An alternative strategy to raise the specific energy is to use multielectron systems. From Figure 1, we observe that it would be difficult to find a +2/+4 couple for which both the +2/+3 and +3/+4 couples are active in the 3–4.5 V window. For a given element, either the +2/+3 couple is of interest but the +3/+4 couple tends to be too high in voltage (e.g., Fe, Mn, Co, or Cr) or the +3/+4 couple is lower than 4.5 V but the +2/+3 couple is very low (e.g., V and Mo). This voltage issue is one of the fundamental difficulties in the development of high capacity +2/+4 phosphates-based cathodes (e.g., $\text{Li}_2\text{FeP}_2\text{O}_7$,³² $\text{Li}_2\text{MnP}_2\text{O}_7$,^{33,34} $\text{Li}_2\text{FePO}_4\text{F}$,³⁵ and $\text{Li}_2\text{CoPO}_4\text{F}$ ³⁶). Only in

certain rare crystal structures can the $\text{Mn}^{3+}/\text{Mn}^{4+}$ couple be active at a voltage lower than 4.5 V as in the recently proposed $\text{Li}_3\text{Mn}(\text{CO}_3)(\text{PO}_4)$ carbonophosphate.^{37–39} On the other hand, vanadium- and molybdenum-based compounds suffer from lower maximal gravimetric capacity as one-electron couples but have a unique potential for multielectron activity in phosphates (i.e., $\text{Mo}^{3+}/\text{Mo}^{6+}$ and $\text{V}^{3+}/\text{V}^{5+}$) within a 3–4.5 V voltage window. Previous work, focusing mainly on the vanadium chemistries, has already been conducted (e.g., $\text{Li}_3\text{V}_2(\text{PO}_4)_3$ NASICON,^{40–42} $\text{Li}_5\text{V}(\text{PO}_4)_2\text{F}_2$,⁴³ and $\text{Li}_9\text{M}_3(\text{P}_2\text{O}_7)_3(\text{PO}_4)_2$ ⁴⁴ with $\text{M} = \text{V}$ or Mo) but a vanadium- or molybdenum-based two-electron cathode with a crystal structure allowing, high capacity, fast and highly reversible Li extraction and insertion has not been found yet.

3.2. Computed Voltages and Stability of LiMX Compounds with $\text{X} = \text{PO}_4\text{F}$, $\text{PO}_4(\text{OH})$, or P_2O_7 . The voltage mismatch between +2/+3 and +3/+4 couples in phosphates is unfortunate, because it excludes from practical applications several known phosphate-based crystal structures that have been shown to be electrochemically active for reversible lithium insertion using a +2/+3 couple as well as for delithiation using the +3/+4 couple. There are several crystal structures of general formula LiMX (with $\text{X} = \text{PO}_4\text{F}$, $\text{PO}_4(\text{OH})$, or P_2O_7 , where M is a +3 redox active metal) that have been shown to accommodate a significant amount of Li during insertion ($\text{LiMX} + x \text{Li} \rightarrow \text{Li}_{1+x}\text{MX}$), as well as allowing topotactic delithiation without major structural instability ($\text{LiMX} \rightarrow \text{Li}_{1-y}\text{MX} + y \text{Li}$). For the fluorophosphate tavorite LiMPO_4F , reversible processes have been demonstrated for the insertion reaction in the iron, titanium, and vanadium forms and for delithiation in the titanium and vanadium forms.^{45–48} Similarly, the tavorite hydroxyphosphate $\text{LiM}(\text{PO}_4)(\text{OH})$ can insert one Li atom, as shown recently in the iron version,⁴⁹ and might, with the adequate +3/+4 couple, be delithiated to remove one Li atom. The LiMP_2O_7 structure, on the other hand, is known to be electrochemically active for the insertion of 0.5 Li per transition metal in LiFeP_2O_7 ,⁵⁰ LiTiP_2O_7 , and LiVP_2O_7 .⁵¹ In addition, Barker et al. demonstrated full reversible lithium deintercalation from LiVP_2O_7 .⁴⁶ While these three structures have adequate Li sites for insertion and delithiation, and could lead to high theoretical capacities if the two sites per transition metals could be used (up to 224 mAh/g for $\text{LiM}(\text{P}_2\text{O}_7)$, 302 mAh/g for $\text{LiM}(\text{PO}_4)(\text{OH})$, and 299 mAh/g for $\text{LiM}(\text{PO}_4)\text{F}$), so far, they have not been able to deliver this large capacity, because of the voltage mismatch of the +2/+3 and +3/+4 couples. Figure 2 illustrates the voltage mismatch in those structures by showing the computed voltage for common redox couples in the tavorites $\text{LiM}(\text{PO}_4)\text{F}$ (green diamond, \blacklozenge), $\text{LiM}(\text{PO}_4)(\text{OH})$ (blue circle, \bullet) and pyrophosphates $\text{LiM}(\text{P}_2\text{O}_7)$ (red triangle, \blacktriangle).

For all elements except Mo and V, the +3/+4 couple is too high in voltage in all structures. On the other hand, vanadium and molybdenum show a very low voltage for their +2/+3 couples, making pure V or Mo compounds operate on a low average voltage with a very important voltage step between the two couples. The average voltage obtained on a large pool of phosphates (i.e., compounds belonging to the Li-M-P-O chemical system where M is a redox active element¹⁰) is also indicated by a black cross (\times) in Figure 2, and the computed voltages are provided in Table 1 as well.

Figure 2 shows some trends in voltage among the different structures considered. For all +2/+3 couples, the pyrophosphates (red triangles, \blacktriangle) have the highest voltage followed by

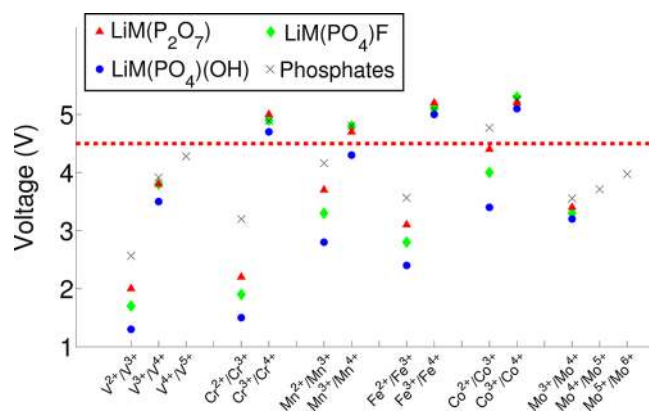


Figure 2. Computed voltages for different redox couples active in $\text{LiM}(\text{P}_2\text{O}_7)$ (red triangles, \blacktriangle), $\text{LiM}(\text{PO}_4)\text{F}$ (green diamonds, \blacklozenge), and $\text{LiM}(\text{PO}_4)(\text{OH})$ structures (blue circles, \bullet). The average voltage for delithiation in phosphates (i.e., compounds containing a P^{5+} ion) is also indicated by a black cross (\times).¹⁰ The red dashed line indicates the approximate voltage stability limit in commercial electrolyte.

the fluorophosphates (green diamonds, \blacklozenge) and the hydroxyphosphates (blue circles, \bullet). The fluorophosphates are expected to lie higher in voltage due to the influence of fluorine, and the pyrophosphates (P_2O_7 groups) have already been shown to have slightly higher voltages than orthophosphates (PO_4 groups).¹⁰ We also observe that the +2/+3 couples are all lower in voltage than the average value given in our previous high-throughput study (black crosses (\times) in Figure 2). This is consistent with the average values in ref 10 being from delithiation of a stable +2 compound using the +2/+3 couple, while the +2/+3 voltages in this work are obtained by insertion into a stable +3 compound. As the voltage is directly proportional to the difference in energy between the charged (delithiated) and discharged (lithiated) state, compounds that are stable in their charged state will show lower voltages than compounds stable in their discharged states, for the same redox couple.

The computed voltages can be compared to experiments for the few compounds with reported electrochemical measurement. Insertion in the $\text{LiM}(\text{P}_2\text{O}_7)$ structure has been reported experimentally at 2.0 V for vanadium⁵¹ and at 2.9 V for iron.⁵⁰ Both are in agreement with our computed values of 2.0 V and 3.1 V, respectively. The delithiation of the $\text{LiV}(\text{P}_2\text{O}_7)$ compound, on the other hand, is reported to be between 4.1 and 4.0 V. This is slightly higher than the computed value of 3.8 V.⁴⁶ The manganese version of the pyrophosphate, $\text{LiMn}(\text{P}_2\text{O}_7)$, is known but no electrochemistry has been reported on this material so far. The chromium pyrophosphate $\text{LiCr}(\text{P}_2\text{O}_7)$ was reported to be electrochemically active for the $\text{Cr}^{3+}/\text{Cr}^{4+}$ couple between 3.1 V and 3.5 V,⁵⁴ which is in large disagreement with the computations (5 V). However, the experimental study did not prove that the electrochemical process was the result of topotactic insertion. Marx et al. measured insertion into $\text{LiFe}(\text{PO}_4)(\text{OH})$ between 2.6 V and 2.3 V, in agreement with our computed value of 2.4 V, and reported no activity up to 4.7 V for the delithiation (activation of the $\text{Fe}^{3+}/\text{Fe}^{4+}$ couple), in agreement as well with our computed value of 5 V.⁴⁹ Surprisingly, the iron version is the only hydroxyphosphate tavorite with a reported electrochemical measurement. The vanadium $\text{LiV}(\text{PO}_4)(\text{OH})$ has been patented as a cathode by Barker et al.,⁵² but, to the best of our knowledge, no report on this material is present in the

Table 1. Stability of Known and Predicted +3 Compounds in $\text{LiM}(\text{P}_2\text{O}_7)$, $\text{LiM}(\text{PO}_4)\text{F}$, and $\text{LiM}(\text{PO}_4)(\text{OH})^a$

formula	structure prototype	space group	experimental information	energy above hull (meV/atom)	$\text{Li}_1 \rightarrow \text{Li}_2$ (V)	$\text{Li}_1 \rightarrow \text{Li}_0$ (V)
$\text{LiV}(\text{P}_2\text{O}_7)$	$\text{LiIn}(\text{P}_2\text{O}_7)$	$P12_11$ (4)	93021	0	2.0	3.8
$\text{LiMn}(\text{P}_2\text{O}_7)$	$\text{LiIn}(\text{P}_2\text{O}_7)$	$P12_11$ (4)	415153	0	3.7	4.7
$\text{LiCr}(\text{P}_2\text{O}_7)$	$\text{LiIn}(\text{P}_2\text{O}_7)$	$P12_11$ (4)	240965	0	2.2	5.0
$\text{LiFe}(\text{P}_2\text{O}_7)$	$\text{LiIn}(\text{P}_2\text{O}_7)$	$P12_11$ (4)	63509	0	3.1	5.2
$\text{LiMo}(\text{P}_2\text{O}_7)$	$\text{LiIn}(\text{P}_2\text{O}_7)$	$P12_11$ (4)	68522	0	0.9	3.4
$\text{LiCo}(\text{P}_2\text{O}_7)$	$\text{LiIn}(\text{P}_2\text{O}_7)$	$P12_11$ (4)	none	0	4.35	5.27
$\text{LiV}(\text{PO}_4)(\text{OH})$	$\text{LiFe}(\text{PO}_4)(\text{OH})$	$P\bar{1}$ (2)	patent (ref 52)	0	1.3	3.5
$\text{LiMn}(\text{PO}_4)(\text{OH})$	$\text{LiFe}(\text{PO}_4)(\text{OH})$	$P\bar{1}$ (2)	67495	8	2.8	4.3
$\text{LiCr}(\text{PO}_4)(\text{OH})$	$\text{LiFe}(\text{PO}_4)(\text{OH})$	$P\bar{1}$ (2)	none	0	1.5	4.7
$\text{LiFePO}_4(\text{OH})$	$\text{LiFe}(\text{PO}_4)(\text{OH})$	$P\bar{1}$ (2)	250117	0	2.4	5.0
$\text{LiMo}(\text{PO}_4)(\text{OH})$	$\text{LiFe}(\text{PO}_4)(\text{OH})$	$P\bar{1}$ (2)	none	0	0.2	3.2
$\text{LiCo}(\text{PO}_4)(\text{OH})$	$\text{LiFe}(\text{PO}_4)(\text{OH})$	$P\bar{1}$ (2)	none	0	3.4	5.1
$\text{LiV}(\text{PO}_4)\text{F}$	$\text{LiAl}(\text{PO}_4)\text{F}$	$P\bar{1}$ (2)	literature (ref 45)	0	1.7	3.8
$\text{LiMn}(\text{PO}_4)\text{F}$	$\text{LiAl}(\text{PO}_4)\text{F}$	$P\bar{1}$ (2)	none	0	3.3	4.8
$\text{LiCr}(\text{PO}_4)\text{F}$	$\text{LiAl}(\text{PO}_4)\text{F}$	$P\bar{1}$ (2)	patent (ref 53)	0	1.9	4.9
$\text{LiFe}(\text{PO}_4)\text{F}$	$\text{LiAl}(\text{PO}_4)\text{F}$	$P\bar{1}$ (2)	literature (ref 47)	0	2.8	5.1
$\text{LiMo}(\text{PO}_4)\text{F}$	$\text{LiAl}(\text{PO}_4)\text{F}$	$P\bar{1}$ (2)	none	2	1.0	3.3
$\text{LiCo}(\text{PO}_4)\text{F}$	$\text{LiAl}(\text{PO}_4)\text{F}$	$P\bar{1}$ (2)	none	0	4.0	5.3

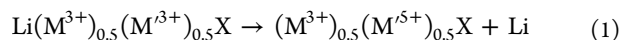
^aComputed voltages for the insertion of one electron ($\text{Li}_1 \rightarrow \text{Li}_2$) and removal of one electron ($\text{Li}_1 \rightarrow \text{Li}_0$) are also indicated. When previously existing experimental information is present in the Inorganic Crystal Structure Database (ICSD), we provide the ICSD reference number. For compounds with no corresponding entry in the ICSD but information from the literature or patents, we referred to those. We note that the ICSD refers to a $\text{LiFe}(\text{PO}_4)\text{F}$ entry, but this entry is from a computational paper and a delithiated structure of $\text{Li}_2\text{Fe}(\text{PO}_4)\text{F}$.

scientific literature. No report of delithiation or insertion could be found for the known $\text{LiMn}(\text{PO}_4)(\text{OH})$; only a lithium diffusion measurement exists.^{55–57} From the three families studied, the fluorophosphate tavorite is, by far, the one receiving the most interest from the battery community. Very recently, Ramesh et al. reported electrochemical Li insertion into $\text{LiFe}(\text{PO}_4)\text{F}$ at 2.9 V, in agreement with the computed voltage of 2.8 V.⁴⁷ The voltages for vanadium tavorite $\text{LiV}(\text{PO}_4)\text{F}$ have been measured at 4.2 V for the delithiation and 1.8 V for insertion.^{45,58} While the insertion value is close to the computed value of 1.7 V, the computed voltage for delithiation underestimates the experimental value by 0.4 V, which is larger than the usual GGA+*U* error. All of the values that we have obtained are consistent with our previous computational work on tavorites.¹⁹

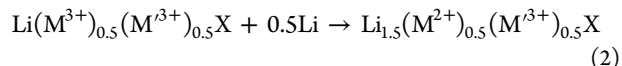
In addition to providing interstitial sites for Li insertion, and stability upon lithium removal, the tavorites $\text{LiM}(\text{PO}_4)\text{F}$ and $\text{LiM}(\text{PO}_4)(\text{OH})$ as well as the $\text{LiM}(\text{P}_2\text{O}_7)$ structures are very common and are stable for almost any +3 redox active transition metal. Table 1 shows the energy above the hull (i.e., the energy for decomposition to more stable phases at 0 K) for V, Mn, Cr, Fe, Co, and Mo in the three structures of interest. Some of these compounds are not present in the Inorganic Crystal Structure Database (ICSD) and might never have been previously synthesized, but all of them are within 10 meV/atom from decomposition to other phases, which is well within the typical density functional theory (DFT) error.³⁷

3.3. Transition-Metal Mixing Strategy To Increase Theoretical Capacity. The main idea behind our mixing strategy is to form $\text{LiM}_{0.5}\text{M}'_{0.5}\text{X}$ compounds (with $\text{X} = \text{P}_2\text{O}_7$, $\text{PO}_4(\text{OH})$, or PO_4F , and $\text{M} = \text{Fe}, \text{Mn}, \text{Cr},$ or Co , and $\text{M}' = \text{V}$ or Mo) in crystal structures known to be good intercalation cathodes. By mixing an ionic species that could be reduced to +2 at a high enough voltage ($\text{M} = \text{Fe}^{3+}, \text{Mn}^{3+}, \text{Cr}^{3+},$ or Co^{3+}) with an ionic species ($\text{M}' = \text{V}^{3+}$ or Mo^{3+}) capable of being oxidized from +3 to either +5 or +6 at a voltage lower than 4.5 V (see Figure 2), we can, in theory, achieve a higher capacity

than for the compounds composed of one active element. Indeed, using the possibility for V^{3+} and Mo^{3+} to oxidize up to V^{5+} and Mo^{5+} at moderate voltage, full deintercalation of the $\text{LiM}_{0.5}\text{M}'_{0.5}\text{X}$ solid solution can be expected through



In addition, lithium insertion through reduction of the M^{3+} species is still possible, via



The full reaction corresponds to the exchange of 1.5 electrons per transition metal and makes the maximal theoretical capacity achievable (up to 227 mAh/g) higher than that observed when using a one-electron couple. This strategy addresses the problem that these structures only accommodate $\text{M}^{2+}/\text{M}^{3+}/\text{M}^{4+}$ cations when made with a single metal but that no transition metal has an appropriate +2/+3 and +3/+4 redox couple. By combining the high-voltage two-electron redox activity of V or Mo with a single electron of a +2/+3 couple, high capacity in a reasonable voltage range can be achieved.

The mixing process is illustrated in Figure 3 for $\text{LiM}(\text{P}_2\text{O}_7)$ as an example. Individually, the manganese and vanadium compounds suffer from limited useful capacity. Delithiation from the manganese compound $\text{LiMn}(\text{P}_2\text{O}_7)$ requires too high a voltage (4.7 V) and, therefore, the compound has a limited useful capacity of 113 mAh/g (by insertion of one Li using the $\text{Mn}^{2+}/\text{Mn}^{3+}$ couple). On the other hand, $\text{LiV}(\text{P}_2\text{O}_7)$ could, in theory, both insert and remove one Li atom per V atom. However, the insertion process occurs at low voltage, making two-electron capacity only reachable with an important voltage step (1.8 V) and with a low average voltage (2.9 V). Both these characteristics are detrimental for practical battery cathodes. By mixing Mn and V atoms on the transition metal site and forming $\text{LiMn}_{0.5}\text{V}_{0.5}(\text{P}_2\text{O}_7)$, we can design a cathode with enhanced theoretical capacity (169 mAh/g), a lower voltage step (0.8 V), and a higher average voltage (4 V). By using the

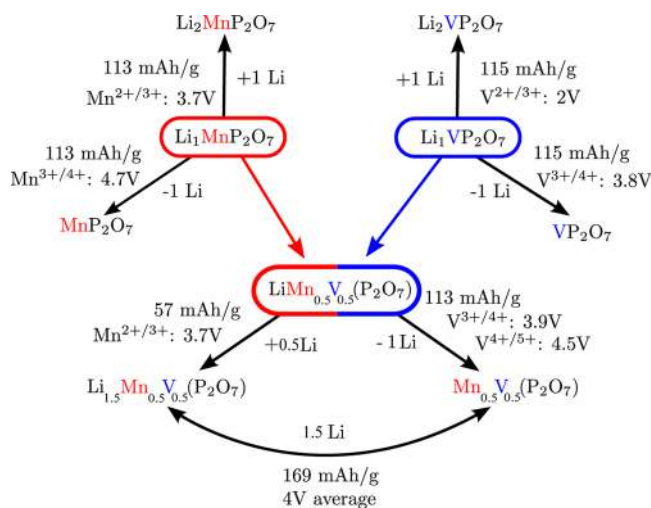


Figure 3. Scheme for the transition-metal mixing strategy. The mixing of Mn and V on the transition-metal site of $\text{LiM}(\text{P}_2\text{O}_7)$ is taken as an example. All reported voltage values are from GGA+*U* computations.

$\text{Mn}^{2+}/\text{Mn}^{3+}$, $\text{V}^{3+}/\text{V}^{4+}$, and $\text{V}^{4+}/\text{V}^{5+}$ couples, a theoretical capacity corresponding to a 1.5 electrons per transition metal is achievable.

In summary, our mixing strategy requires a structural framework prone to accommodate multiple Li atoms per transition metal, a metal active at a high voltage on its 2+/3+ couple (e.g., Mn, Fe or Co), and a metal with a multielectron couple active at a voltage lower than 4.5 V (e.g., V or Mo). By mixing those two active metals in such a crystal structure, we can design cathode materials activating more than one Li atom per transition metal in a reasonable voltage range, thereby offering significantly higher usable capacities than the single-metal compounds.

3.4. Applying the Mixing Strategy to Vanadium-Based Compounds. Using the general strategy outlined in the previous section, we present the computational results for mixing of *M* atoms (*M* = Cr, Fe, Mn, Co) with V atoms in $\text{LiM}_{0.5}\text{V}_{0.5}\text{X}$ (with *X* = P_2O_7 , $\text{PO}_4(\text{OH})$, or PO_4F). Figure 4 shows a voltage versus capacity plot for the different pure and mixed compounds in the LiMPO_4F (green diamond, \blacklozenge), $\text{LiMPO}_4(\text{OH})$ (blue circle, \bullet), and $\text{LiM}(\text{P}_2\text{O}_7)$ (red triangle, \blacktriangle) crystal structures. Single transition-metal compounds are marked by their transition metal. The average voltage and capacity of mixed transition-metal compounds is marked by the two mixed transition metals separated by a dash. Isolines of specific energy are drawn in dark green. Only capacities deliverable with a computed voltage lower than 4.6 V and with voltage steps <2 V are included in the figure. Most pure compounds do not show high enough capacity to reach specific energies of interest (>600 Wh/kg, as in LiFePO_4) but the mixed transition-metal compounds can lead to higher specific energies.

The only single transition-metal compound with a potential for high specific energy in the 2–4.5 V voltage window is $\text{LiMn}(\text{PO}_4)\text{OH}$ (denoted by the blue circle marked Mn at 300 mAh/g). This is the only compound where the +3/+4 couple is low enough to not compromise the electrolyte stability (4.3 V), while the +2/+3 couple remains relatively high at 2.8 V (see Figure 2). Surprisingly, no electrochemical testing for this known material has been reported. Only structural and Li diffusion experimental data are available.^{55–57}

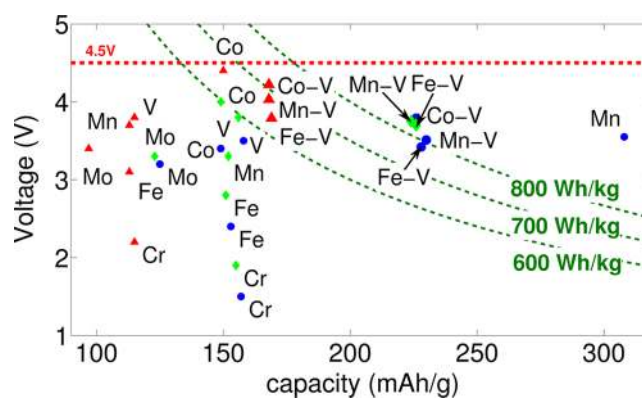


Figure 4. Voltage versus capacity plot for pure and mixed compounds ($\text{LiM}_{0.5}\text{V}_{0.5}\text{X}$ (with *X* = P_2O_7 , $\text{PO}_4(\text{OH})$, or PO_4F)). Favorites LiMPO_4F (green diamonds, \blacklozenge), $\text{LiMPO}_4(\text{OH})$ (blue circles, \bullet) and LiMP_2O_7 (red triangles, \blacktriangle). Single transition-metal compounds are marked by their transition metal, and mixed compounds are marked by the two mixed transition metals separated by a dash. Isolines of specific energy are drawn in dark green. For the sake of readability, the average voltage is plotted when the voltage profile contains several voltage steps. The exact voltage steps can be obtained in Table 2.

The pyrophosphate-based compounds show lower capacities than the fluorophosphate and hydroxyphosphate favorites. This is due to the smaller charge to mass ratio of the P_2O_7 group compared to PO_4F and $\text{PO}_4(\text{OH})$. For all chromium-based mixtures, the $\text{Cr}^{2+}/\text{Cr}^{3+}$ is so close in voltage to the $\text{V}^{2+}/\text{V}^{3+}$ couple that it does not perform significantly better than the pure vanadium system. The voltage, specific energy, and energy density data is also provided in Table 2.

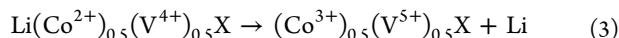
To be of interest, the proposed mixed transition-metal compounds need to be stable enough energetically to be synthesizable. While mixing of the transition metals will be promoted by entropic contributions at the high temperatures often used in synthesis, it is of interest to study the energetic component of the mixing. Therefore, we can compute the energy above the hull for all the mixed transition-metal compounds. The energy above the hull indicates the driving force for possible decomposition into more-stable phases at 0 K: the higher the energy above the hull, the less stable the material. Stable compounds at 0 K have an energy above the hull of 0 meV/atom. Table 2 presents, along with electrochemical property, indications about the stability of the mixed compounds by providing their energy above the hull per atom. Most of the mixtures are energetically favorable with relatively low energies above the hull, as expected for the mixing of transition metals forming similar crystal structures. Across the three crystal structures, the least-stable mixtures are the manganese-based ones. The unfavorable energetics for Mn and V mixing is quite surprising for two ions with similar ionic radii (0.645 Å for Mn^{3+} high-spin and 0.69 Å for V^{3+})⁵⁹ and a strong tendency to form similar structures, as indicated by data mining.⁶⁰ However, even though the pure form of a given Mn^{3+} could be isostructural with the V^{3+} parent compounds, it is possible that the strong Jahn–Teller activity of Mn^{3+} leads to large distortion energy of the octahedra around V^{3+} when both metals are mixed in a structure.

We verified the valence state of the transition metals in the mixed compounds by computing the magnetic moments on vanadium and the other transition metal. For all but Co-based compounds, the magnetic moment on vanadium is $\sim 1.9 \mu_B$, indicating a V^{3+} oxidation state. In the case of cobalt, the lower

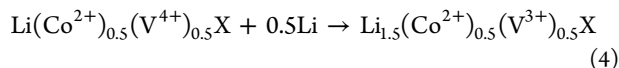
Table 2. Computed Electrochemical and Stability Properties for the Different Designed $\text{LiM}_{0.5}\text{V}_{0.5}\text{X}$ Vanadium-Based Compounds

formula	energy above hull (meV/atom)	Voltage (V)		capacity (mAh/g)	specific E (Wh/kg)	E density (Wh/L)
		$\text{Li}_1 \rightarrow \text{Li}_{1.5}$	$\text{Li}_1 \rightarrow \text{Li}_0$			
$\text{LiMn}_{0.5}\text{V}_{0.5}(\text{P}_2\text{O}_7)$	6	3.62	3.95; 4.52	169	681	1911
$\text{LiFe}_{0.5}\text{V}_{0.5}(\text{P}_2\text{O}_7)$	0	3.01	3.91; 4.46	169	640	1826
$\text{LiCr}_{0.5}\text{V}_{0.5}(\text{P}_2\text{O}_7)$	0	1.97	3.94; 4.48	170	589	1668
$\text{LiCo}_{0.5}\text{V}_{0.5}(\text{P}_2\text{O}_7)$	2.4	3.57	4.50; 4.50	168	708	2050
$\text{LiMn}_{0.5}\text{V}_{0.5}(\text{PO}_4)(\text{OH})$	22	2.63	3.67; 4.24	229	804	2396
$\text{LiFe}_{0.5}\text{V}_{0.5}(\text{PO}_4)(\text{OH})$	0	2.16	3.51; 4.59	228	783	2370
$\text{LiCr}_{0.5}\text{V}_{0.5}(\text{PO}_4)(\text{OH})$	0	1.2	3.55; 4.72	231	730	2186
$\text{LiCo}_{0.5}\text{V}_{0.5}(\text{PO}_4)(\text{OH})$	15	2.44	4.36; 4.57	226	858	2685
$\text{LiMn}_{0.5}\text{V}_{0.5}(\text{PO}_4)\text{F}$	20	3.19	3.7; 4.37	226	849	2668
$\text{LiFe}_{0.5}\text{V}_{0.5}(\text{PO}_4)\text{F}$	0	2.88	3.75; 4.48	226	835	2654
$\text{LiCr}_{0.5}\text{V}_{0.5}(\text{PO}_4)\text{F}$	0	1.9	3.81; 4.54	228	780	2467
$\text{LiCo}_{0.5}\text{V}_{0.5}(\text{PO}_4)\text{F}$	5	3.29	4.4; 4.83	223	933	3023

magnetic moment on vanadium indicates a $\text{V}^{4+}-\text{Co}^{2+}$ mixture, rather than a $\text{V}^{3+}-\text{Co}^{3+}$ mixture. Therefore, the cobalt-based compounds react by oxidizing the $\text{V}^{4+}/\text{V}^{5+}$ and $\text{Co}^{2+}/\text{Co}^{3+}$ couples during delithiation:



and have the $\text{V}^{3+}/\text{V}^{4+}$ couple activated during lithium insertion:



This influences the voltage profile and explains the very high voltage for the charge profile (4.83 V) in $\text{LiCo}_{0.5}\text{V}_{0.5}(\text{PO}_4)\text{F}$ due to the activation of Co^{2+} to Co^{3+} and not V^{4+} to V^{5+} .

Comparing the calculated Li extraction voltage of LiVPO_4F (activating $\text{V}^{3+}/\text{V}^{4+}$) with experiment, we pointed out that GGA+*U* underpredicts significantly the voltage (3.8 V instead of 4.2 V). The discrepancy between experimental and computational results unfortunately cast concerns on the very interesting battery properties found in mixed vanadium compounds in the $\text{LiFe}_{0.5}\text{V}_{0.5}(\text{PO}_4)\text{F}$ and $\text{LiMn}_{0.5}\text{V}_{0.5}(\text{PO}_4)\text{F}$ fluorophosphate tavorite. It is possible that the *U* value for V, fitted on oxide reaction energies, might not be adequate on fluorophosphates and the voltage results for the vanadium fluorophosphates, therefore, should be taken with caution.

3.5. Applying the Mixing Strategy to Molybdenum-Based Compounds. Similar to vanadium, molybdenum has both the $\text{Mo}^{3+}/\text{Mo}^{4+}$ and $\text{Mo}^{4+}/\text{Mo}^{5+}$ couples fairly similar in voltages and below 4.5 V in phosphates (see Figures 1 and 2).¹⁰ We applied our mixing strategy to the $\text{LiM}_{0.5}\text{Mo}_{0.5}\text{X}$ (with $\text{X} = \text{P}_2\text{O}_7$, $\text{PO}_4(\text{OH})$, or PO_4F and $\text{M} = \text{Cr}$, Fe , Mn , Co) chemistries. Figure 5 shows a voltage versus capacity plot for the different pure and mixed compounds in the LiMPO_4F (green diamond), $\text{LiMPO}_4(\text{OH})$ (blue circle), and $\text{LiM}(\text{P}_2\text{O}_7)$ (red triangle) tavorite structures. Isolines of specific energy are drawn in dark green. Only capacities deliverable with a computed voltage of <4.6 V and with voltage steps of <2 V are included in the figure. Similar to vanadium, most pure compounds do not show high enough capacity to reach specific energies of interest (>600 Wh/kg, as in LiFePO_4) but the mixed transition-metal compounds can lead to higher specific energies.

The larger weight of molybdenum makes the theoretical gravimetric capacities lower than for the equivalent vanadium-based compound. In addition, molybdenum is active at a lower voltage than vanadium.¹⁰ Both of those effects gives the

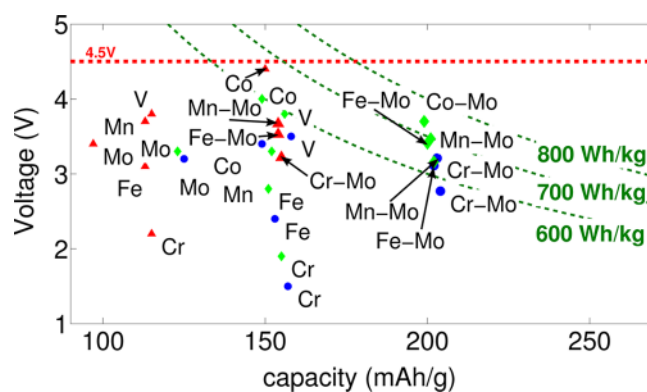


Figure 5. Voltage versus capacity plot for pure and mixed compounds ($\text{LiM}_{0.5}\text{Mo}_{0.5}\text{X}$ (with $\text{X} = \text{P}_2\text{O}_7$ (red triangle, \blacktriangle), $\text{PO}_4(\text{OH})$ (blue circle, \bullet), or PO_4F) (green diamond, \blacklozenge). Single transition-metal compounds are marked by their transition metal when mixtures are marked by the two mixed transition metals separated by a dash. Isolines of specific energy are drawn in dark green. For the sake of readability, the average voltage is plotted when the voltage profile contains several voltage steps. The exact voltage steps can be obtained in Table 3.

molybdenum-based compounds lower specific energies than the vanadium compounds and no mixed pyrophosphate reaches a specific energy of >600 Wh/kg. However, the difference between Mo and V is less pronounced when it comes to the volumetric energy densities (compare Tables 2 and 3).

We verified the valence state of the transition metals in the mixed compounds by computing the magnetic moments on molybdenum and the other transition metal. The mixtures of iron, and chromium with molybdenum show magnetic moments in the range of 1.9–2 μ_B , in agreement with a Mo^{3+} oxidation state. On the other hand, the manganese and cobalt compounds show a magnetic moment of $\sim 2.8 \mu_B$ on Mo, indicating a Mo^{4+} oxidation state. An investigation of the change in magnetic moments during delithiation also showed that, in the case of the Co–Mo compounds, Mo was oxidized up to +6 (with Co remaining +2) but on the other hand, in the case of Mn–Mo mixtures, Mo was oxidized up to +5 and Mn was oxidized to +3, in agreement with the higher voltage associated with the $\text{Co}^{2+}/\text{Co}^{3+}$ redox couple, compared to the $\text{Mn}^{2+}/\text{Mn}^{3+}$ couple.

The $\text{LiCo}_{0.5}\text{Mo}_{0.5}(\text{PO}_4)\text{F}$ compound is of interest, even though cobalt is not active (remains +2). By taking advantage

Table 3. Computed Electrochemical and Stability Properties for the Different Designed LiM_{0.5}Mo_{0.5}X Molybdenum-Based Compounds

formula	energy above hull (meV/atom)	Voltage (V)		capacity (mAh/g)	specific E (Wh/kg)	E density (Wh/L)
		Li ₁ → Li _{1.5}	Li ₁ → Li ₀			
LiMn _{0.5} Mo _{0.5} (P ₂ O ₇)	2	3.01	3.92; 3.92	154	567	1671
LiFe _{0.5} Mo _{0.5} (P ₂ O ₇)	0	3.03	3.59; 3.97	154	544	1642
LiCr _{0.5} Mo _{0.5} (P ₂ O ₇)	0	2.1	3.6; 3.98	155	501	1584
LiCo _{0.5} Mo _{0.5} (P ₂ O ₇)	3	3.26	3.77; 5.0	153	614	1878
LiMn _{0.5} Mo _{0.5} (PO ₄)(OH)	14	2.09	3.73; 3.83	203	652	2071
LiFe _{0.5} Mo _{0.5} (PO ₄)(OH)	4	2.16	3.18; 3.98	202	629	2076
LiCr _{0.5} Mo _{0.5} (PO ₄)(OH)	0	1.12	3.22; 3.97	204	567	1854
LiCo _{0.5} Mo _{0.5} (PO ₄)(OH)	18	2.26	3.72; 4.70	201	714	2450
LiMn _{0.5} Mo _{0.5} (PO ₄)F	23	2.86	3.72; 3.86	201	699	2376
LiFe _{0.5} Mo _{0.5} (PO ₄)F	10	2.77	3.38; 4.09	200	683	2365
LiCr _{0.5} Mo _{0.5} (PO ₄)F	3	2.17	3.42; 3.89	202	639	2165
LiCo _{0.5} Mo _{0.5} (PO ₄)F	0	2.61	3.97; 4.54	199	736	2602

Table 4. Computed Electrochemical and Stability Properties for the Different Designed Mo⁴⁺–M²⁺ Compounds

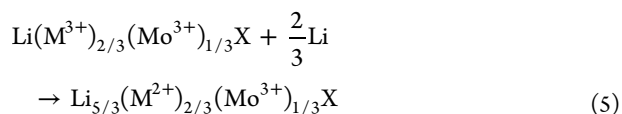
formula	energy above hull (meV/atom)	voltage (V)	capacity (mAh/g)	specific E (Wh/kg)	E density (Wh/L)
LiCo _{0.5} Mo _{0.5} (PO ₄)F	0	2.61; 3.97; 4.54	199	736	2602
LiNi _{0.5} Mo _{0.5} (PO ₄)F	0	2.56; 4.01; 4.59	199	741	2650
LiZn _{0.5} Mo _{0.5} (PO ₄)F	29	2.94; 3.88; 4.18	196	718	2564
LiMg _{0.5} Mo _{0.5} (PO ₄)F	22	2.87; 3.9; 4.26	218	799	2610

Table 5. Electrochemical and Stability Properties for the Different Designed LiM_{2/3}Mo_{1/3}X Molybdenum-Based Compounds

formula	energy above hull (meV/atom)	Voltage (V)		capacity (mAh/g)	specific E (Wh/kg)	E density (Wh/L)
		Li ₁ → Li _{5/3}	Li ₁ → Li ₀			
LiFe _{2/3} Mo _{1/3} (P ₂ O ₇)	0	3.05; 3.05	3.64; 4.01; 5.2	175	664	1958
LiCr _{2/3} Mo _{1/3} (P ₂ O ₇)	0	2.14; 2.14	3.64; 4.06; 4.9	176	596	1720
LiFe _{2/3} Mo _{1/3} (PO ₄)(OH)	4	2.16; 2.21	3.27; 4.02; 4.79	231	761	2396
LiCr _{2/3} Mo _{1/3} (PO ₄)(OH)	1	1.23; 1.23	3.36; 3.82; 4.85	234	680	2127
LiFe _{2/3} Mo _{1/3} (PO ₄)F	12	2.12; 2.89	3.44; 4.42; 5.21	233	829	2724
LiCr _{2/3} Mo _{1/3} (PO ₄)F	0	1.98; 2.14	3.4; 4.09; 4.65	232	755	2463

of the possibility for Mo to be oxidized higher up to 6+, replacing part of the Mo by the lighter Co can improve the theoretical gravimetric capacity. This alternative design strategy can be extended to other +2 ions such as Mg, Zn, or Ni, and computed data for a few of +4/+2 mixed compounds are presented in Table 4. Both the Ni and Co versions are of great interest, in terms of specific energy and energy density, but have a voltage associated with the Mo⁵⁺/Mo⁶⁺ couple that is fairly high. Interestingly, the lower stability of the Mg and Zn mixtures (compared to Ni and Co) lowers the voltage associated with the Mo⁴⁺/Mo⁶⁺ couples and makes this Mo⁵⁺/Mo⁶⁺ voltage less likely to compromise electrolyte stability. However, lower mixing stability indicates that the synthesis of the mixed compound might be more difficult and that the risk for cathode decomposition during cycling is higher.

As molybdenum can be oxidized up to +6, the Mo can be reduced to form a compound Li(M³⁺)_{2/3}(Mo³⁺)_{1/3}X where M is Fe or Cr. The Co³⁺ or Mn³⁺ ions cannot be used, because they would oxidize Mo³⁺. In these compounds, the +2/+3 redox couple is activated in insertion through



The delithiation process can theoretically activate Mo³⁺ to Mo⁶⁺:

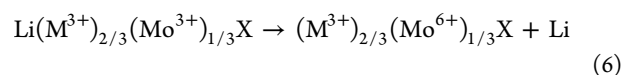


Table 5 presents computed properties for compounds of formula LiM_{2/3}Mo_{1/3}X (with X = P₂O₇, PO₄(OH), or PO₄F and M = Cr, Fe). The lower quantity of molybdenum is favorable to the gravimetric capacity. Unfortunately, the results in Table 5 indicate that the Mo⁵⁺/Mo⁶⁺ couples are too high in voltage in all crystal structures investigated to lead to cathode materials that are compatible with current electrolyte technology.

4. DISCUSSION

The development of high-capacity phosphate-based cathodes has been impeded by the difficulty of finding compounds with both the +2/+3 and +3/+4 redox couples with adequate voltage. In general, transition metals for which the +3/+4 redox couple is below 4.5 V tend to display very low voltages for the +2/+3 redox couple. Therefore, even within crystal structures that are known to separately accommodate Li insertion (+2/+3 redox couple) and Li deinsertion (+3/+4 redox couple), it has been difficult to find a single metal or mixture of metals in a good voltage range. We propose in this work a novel strategy whereby the +2/+3 redox couple of one transition metal is

Table 6. Stability and Electrochemical Computed Data for the Cathode Candidates of Greatest Interest^a

formula	energy above hull (meV/atom)	voltage (V)	capacity (mAh/g)	specific <i>E</i> (Wh/kg)	<i>E</i> density (Wh/L)
Mixtures of Active Elements					
LiFe _{0.5} V _{0.5} (PO ₄)F	0	2.88; 3.75; 4.48	226	835	2654
LiCo _{0.5} V _{0.5} (P ₂ O ₇)	2	3.57; 4.50; 4.50	168	708	2050
LiFe _{0.5} Mo _{0.5} (PO ₄)F	10	2.77; 3.38; 4.09	200	683	2365
LiMn _{0.5} Mo _{0.5} (PO ₄)(OH)	14	2.09; 3.73; 3.83	203	652	2071
LiMn _{0.5} V _{0.5} (PO ₄)F	20	3.19; 3.7; 4.37	226	849	2668
LiMn _{0.5} V _{0.5} (PO ₄)(OH)	22	2.63; 3.67; 4.24	229	804	2396
LiMn _{0.5} Mo _{0.5} (PO ₄)F	23	2.86; 3.72; 3.86	229	699	2376
Mixtures of Active and Inactive Elements					
LiZn _{0.5} Mo _{0.5} (PO ₄)F	29	2.94; 3.88; 4.18	196	718	2564
LiMg _{0.5} Mo _{0.5} (PO ₄)F	22	2.87; 3.9; 4.26	218	799	2610
Previously Known Compounds					
LiMn(PO ₄)(OH)	8	2.8; 4.36	296	1059	3094

^aThe mixtures of active elements are sorted by the stability of the LiM_{0.5}M'_{0.5}X mixed phase.

combined with either the +3/+5 redox couple of V or the +3/+5 or +3/+6 redox couples of Mo. By coupling a single-electron process for one metal with a multielectron process for the other metal, the overall capacity can be increased past that of a one-electron process while retaining good voltage (3–4.5 V) throughout.

Our computational analysis identified several potential novel cathode materials with theoretical specific energy and energy density significantly higher than LiFePO₄, the most developed phosphate cathode material. In Table 6, we list the compounds of greatest interest found by our design strategy. If we take a conservative cutoff on the voltage (4.5 V) and look for materials with a specific energy and energy density significantly larger than that of LiFePO₄ (i.e., > 650 Wh/kg and >2000 Wh/L), we find seven compounds from our strategy of mixing electrochemically active elements, two compounds from an alternative strategy that involves mixing Mo with inactive +2 elements, and one compound previously reported in the literature. If we slightly relax the constraints on the upper voltage limit to 4.6 V, several additional materials become of interest (e.g., LiCo_{0.5}Mo_{0.5}(PO₄)F, LiNi_{0.5}Mo_{0.5}(PO₄)F, LiCo_{0.5}V_{0.5}(PO₄)(OH), LiFe_{0.5}V_{0.5}(PO₄)(OH), and LiMn_{0.5}V_{0.5}(P₂O₇)).

Among the three crystal structure families investigated, the LiMP₂O₇ pyrophosphates show the lowest specific energy and energy density, and most of the pyrophosphate compounds studied are unlikely to be of interest. The vast majority of promising compounds are hydroxyphosphate and fluorophosphate tavorites. In the nonmixed compounds (Table 1), the presence of fluorine in the LiM(PO₄)F compounds raises the delithiation voltage (by 0.23 V, on average, compared to that for LiM(PO₄)OH, and by 0.48 V, on average, for insertion (LiMX → Li₂MX). Not surprisingly, the presence of fluorine raises the voltage due to its higher electronegativity.^{61,62} This fluorine effect is also observed for lithium insertion in the mixed compounds (average increase of 0.72 V from the hydroxy to the fluorine-based tavorites). In the first step of delithiation (LiM_{0.5}M'_{0.5}X → Li_{0.5}M_{0.5}M'_{0.5}X), the voltage of the fluorine tavorites is 0.17 V higher than for the hydroxyphosphate tavorites. However, surprisingly, we predict that the last delithiation step in the mixed compounds (Li_{0.5}M_{0.5}M'_{0.5}X → M_{0.5}M'_{0.5}X) occurs, on average, at the same voltage for the fluorine and hydroxyphosphate tavorites. The average higher voltage in fluorine-based compounds often makes the equivalent fluorophosphate of greater interest, in terms of

specific energy and energy density. For instance, comparing LiFe_{0.5}Mo_{0.5}(PO₄)F and LiFe_{0.5}Mo_{0.5}(PO₄)OH, the fluorophosphate compound provides higher specific energy and energy density, because of the higher voltage in insertion and for the first delithiation step. Of course, other factors not taken into account in our study, such as synthesis conditions, cyclability, or rate capability, could favor one chemistry or the other. The possibility of synthesizing mixed hydroxyphosphates–fluorophosphates could add another design knob of interest for future work.⁶³

Among the different +2/+3 redox couples, our analysis shows that Cr²⁺/Cr³⁺ is always too low to be of interest, in terms of energy density. Mn²⁺/Mn³⁺ and Fe²⁺/Fe³⁺ are similar in terms of voltage, but all the Mn compounds show less favorable mixing energetics with V or Mo.

Comparing the specific energies achievable for vanadium- and molybdenum-based compounds, the V compounds outperform the Mo systems. For instance, the vanadium fluorophosphate, LiFe_{0.5}V_{0.5}(PO₄)F, has one of the largest specific energies among our set of compounds. However, it should be noted that the one data point we have for comparison with experiments indicates that our GGA+*U* computations might underestimate voltages in vanadium fluorophosphates. For example, our computations on LiV(PO₄)F using *U* = 3.1 eV underestimates the voltage by ~0.3–0.4 V, compared to experiment. We estimate that a more accurate voltage for the last delithiation step of LiFe_{0.5}V_{0.5}(PO₄)F (i.e., Li_{0.5}Fe_{0.5}V_{0.5}(PO₄)F → Fe_{0.5}V_{0.5}(PO₄)F), would be ~4.89 V (computed using a value of *U* = 4.4 eV for vanadium, which reproduces the experimental voltage of LiV(PO₄)F). We expect that a similar issue might be present for the Mn–V fluorophosphate material (i.e., LiMn_{0.5}V_{0.5}(PO₄)F). This variation in the “optimal” *U* value is of some concern, as the general strategy for predicting voltages has been to fit a *U* value using experimental binary oxide formation enthalpy and using this *U* value in other chemistries. The only issues the authors had been aware of in this matter is the inaccuracies of the Co *U* value obtained on binary oxide values in phosphates.¹⁰ Hybrid functionals are an alternative approach to GGA+*U* also designed to correct for the spurious self-interaction present in standard DFT. Recently, the Haynes–Scuseria–Erzerhoff (HSE) functional has been shown to perform similarly well than GGA+*U* in predicting voltages but at a higher computational cost.^{64,65} In the specific case of LiV(PO₄)F, using HSE leads to a computed delithiation voltage of 4.16 V in very close

agreement with experiment (4.2 V). However, it is not possible at this stage to conclude if the better performance of HSE is coincidental or the sign of a more general trend.

The Mo-based mixed compounds show a slightly lower voltage and lower gravimetric capacity due to the larger weight of Mo. However, there are a few very competitive Mo-based compounds in our set. We find, for example, that the favorite fluorophosphate Fe–Mo mixed compound ($\text{Li}_{0.5}\text{Fe}_{0.5}\text{Mo}_{0.5}(\text{PO}_4)\text{F}$) is of greatest interest with high stability as a mixture, as well as high specific energy and energy density (683 Wh/kg and 2365 Wh/L, respectively). We should note that, while the specific energy is not as competitive as that for vanadium, the volumetric energy density is very attractive (25% higher than LiFePO_4).

In addition to compounds developed by mixing active elements, an alternative strategy was also presented that involved the mixing of an inactive +2 metal with Mo. Although the compound with the most favorable transition-metal mixing, $\text{LiCo}_{0.5}\text{Mo}_{0.5}(\text{PO}_4)\text{F}$, has a last voltage step (4.54 V) in the delithiation profile that could be worrisome for the electrolyte stability, we found $\text{LiMg}_{0.5}\text{Mo}_{0.5}(\text{PO}_4)\text{F}$ to have a less-favorable mixing tendency but with a more attractive last voltage step (4.29 V).

In addition to voltage, specific energy, and energy density, the safety of charged cathode materials is paramount. Since safety can be linked to the thermal stability versus oxygen release of the charged electrode, a scheme based on DFT computations has been recently developed to evaluate the intrinsic thermal stability of a cathode material by computing the oxygen chemical potential for oxygen release.²⁹ Materials with a high oxygen chemical potential for oxygen release will be less thermally stable. From our previous work, we know that the targeted oxidation states in the charged cathode during our design (i.e., V^{5+} , Mo^{5+} , or Mo^{6+}) tend to be intrinsically thermally stable and are associated with low chemical potential for oxygen release.¹⁰ To verify that we indeed designed “safe” cathode materials, we computed the oxygen chemical potential for oxygen release from all the candidate compounds of greatest interest. Figure 6 shows the oxygen chemical potential in the fully delithiated (charged state) versus the specific energy for a few known cathode materials (denoted by black squares, ■), and for our candidate compounds present in Table 6 (green diamond (◆) for $\text{LiM}(\text{PO}_4)\text{F}$, blue circles (●) for $\text{LiM}(\text{PO}_4)(\text{OH})$, and red triangles (▲) for LiMP_2O_7), the inverse correlation between specific energy and safety can be directly observed, with the safest materials (LiFePO_4) being the lowest in specific energy and the least-safe materials (the layered nickel and cobalt oxides) being the highest in specific energy. As pointed out early on by Huggins and co-workers,⁹ and confirmed by more recent computational studies,¹⁰ higher voltage (and therefore higher specific energies) often implies lower thermal stability. The black dashed line in Figure 6 serves as a guide to the eye for the current specific energy versus safety trends in cathode materials of current interest. Most of the compounds proposed in this paper are situated to the right of the dashed line, and are in the region where higher specific energies are obtained without compromising the thermal stability too much.

Our work only screened based on a few necessary battery properties but did not study all aspects of a good battery material. For instance, barriers for lithium diffusion, which are important in terms of rate capability, have not been computed. Our recent computational study showed that the fluorophos-

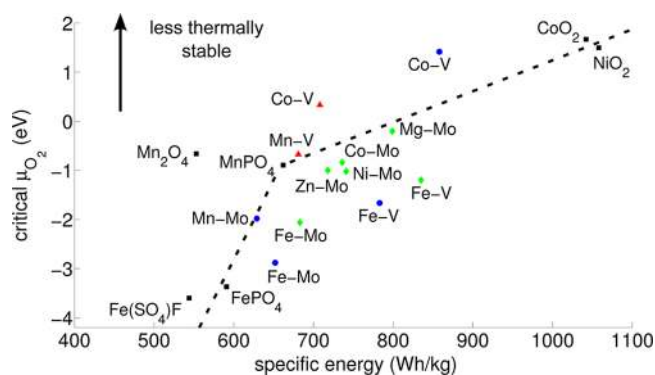


Figure 6. Critical oxygen chemical potential versus theoretical specific energy for the charged state of some known cathode materials (black squares, ■) and for the proposed mixed transition-metal compounds (green diamonds (◆) for $\text{LiM}(\text{PO}_4)\text{F}$ compounds, blue circles (●) for $\text{LiM}(\text{PO}_4)(\text{OH})$, and red triangles (▲) for LiMP_2O_7). The known compounds are LiMn_2O_4 spinel, LiMnPO_4 and LiFePO_4 olivine, LiFeSO_4F avorite, and the layered LiCoO_2 and LiNiO_2 . Materials with a high oxygen chemical potential for oxygen release will be less thermally stable. All results are from GGA+*U* computations. The black dashed line is present to guide the eye. Any new material must be on the right side of this boundary to show an improvement in thermal stability in the charged state or in specific energy, compared to known materials.

phosphateavorites (and especially LiVPO_4F) can have very low lithium migration barriers.¹⁹ Therefore, the fluorophosphate compounds that we propose (e.g., $\text{LiMg}_{0.5}\text{Mo}_{0.5}(\text{PO}_4)\text{F}$ and $\text{LiFe}_{0.5}\text{Mo}_{0.5}(\text{PO}_4)\text{F}$) could form high-energy-density, high-safety, and high-rate cathode materials.

In addition to the mixed compounds, we found one nonmixed compound showing, according to computations, a surprising potential for two-electron redox capacity. $\text{LiMn}(\text{PO}_4)(\text{OH})$ is predicted to be able to insert one Li atom at a voltage of 2.8 V while deintercalating at 4.3 V. The theoretical specific energy and energy density are extremely large (1065 Wh/kg and 3082 Wh/L, respectively). A phosphate-based cathode activating the $\text{Mn}^{3+}/\text{Mn}^{4+}$ couple at a potential lower than 4.5 V is rare but not impossible, as shown by our recent work on $\text{Li}_3\text{Mn}(\text{CO}_3)(\text{PO}_4)$.^{37,38} There are a few reports on $\text{LiMn}(\text{PO}_4)(\text{OH})$;^{55–57} however, no electrochemical measurements have been reported, and this compound might be worthy of electrochemical investigation.

Although we illustrated our mixing strategy with specific crystal structures, the approach can be used on other phosphate materials. For instance, we recently presented the $\text{Li}_3\text{Mo}_2(\text{PO}_4)_3$ NASICON as an interesting cathode material with a somewhat low theoretical capacity of 161 mAh/g.¹⁰ On the other hand, $\text{Li}_3\text{Fe}_2(\text{PO}_4)_3$ NASICON is a well-known material in which two additional Li atoms per formula unit can be inserted but cannot be delithiated, because of the high voltage of the $\text{Fe}^{3+}/\text{Fe}^{4+}$ couple.^{10,40} Using the potential for Mo oxidation up to +6, we can propose a $\text{Li}_3\text{MoFe}(\text{PO}_4)_3$ mixed compound that can be fully delithiated (up to Mo^{6+} in $\text{MoFe}(\text{PO}_4)_3$) and inserted up to one Li atom per formula unit (reducing Fe^{3+} to Fe^{2+} and forming $\text{Li}_4\text{MoFe}(\text{PO}_4)_3$). The capacity of this compound would be ~230 mAh/g. In addition, the mixing strategy can also be used to propose new compounds in chemistries other than phosphates. The chemistries of special interest will be chemistries with high inductive effects that make the +3/+4 couple too high in

voltage, compared to the electrolyte stability window (e.g., fluoropolyanions, sulfates, and fluorides).

5. CONCLUSION

Finding phosphates-based multiple-electron cathode materials active within the stability voltage window of commercial electrolytes is challenging. Toward this goal, we proposed a design strategy based on mixing transition metals in crystal structures known to reversibly accommodate Li in insertion and in delithiation. By mixing elements electrochemically active at a reasonably high voltage on the +2/+3 couples (e.g., Fe) with elements active on the +3/+5 or +3/+6 (i.e., V and Mo) couples within the electrolyte voltage window, we showed that high-capacity multielectron cathodes can be designed. We applied our mixing strategy to a few examples in the phosphate, fluorophosphate, and hydroxyphosphate chemistries and we identified several compounds as materials of interest with promising properties, in terms of voltage, specific energy, energy density, and safety. We hope this computational analysis will motivate experimentalists to synthesize and test these novel cathode candidates electrochemically.

AUTHOR INFORMATION

Corresponding Author

*Tel.: 617-253-1581. Fax: 617-258-6534. E-mail: gceder@MIT.EDU.

Present Addresses

[†]Institut de la Matière Condensée et des Nanosciences (IMCN), European Theoretical Spectroscopy Facility (ETSF), Université Catholique de Louvain, Louvain-la-Neuve, Belgium.

[‡]Computational Research Division, Lawrence Berkeley National Laboratory, Berkeley, CA, USA.

[§]Department of Materials Science and Engineering, Johns Hopkins University, Baltimore, MD, USA.

Notes

The authors declare no competing financial interest.

ACKNOWLEDGMENTS

The authors would like to acknowledge Bosch and Umicore for financial support. This work was also supported in part by the Assistant Secretary for Energy Efficiency and Renewable Energy, Office of Vehicle Technologies of the U.S. Department of Energy (under Contract No. DE-AC02-05CH11231, under the Batteries for Advanced Transportation Technologies (BATT) Program Subcontract No. 6806960), and by the MRSEC Program of the National Science Foundation (under Award No. DMR-0819762). G.H. acknowledges the FNRS-FRS for financial support under a "Chargé de recherche" grant. A.J. acknowledges funding through the U.S. Government (under Contract No. DE-AC02-05CH11231) and the Luis W. Alvarez Fellowship in Computational Science.

REFERENCES

- (1) Ellis, B. L.; Lee, K. T.; Nazar, L. F. *Chem. Mater.* **2010**, *22*, 691–714.
- (2) Whittingham, M. S. *Chem. Rev.* **2004**, *104*, 4271–4302.
- (3) Whittingham, M. *Proc. IEEE* **2012**, *100*, 1518.
- (4) Padhi, A.; Nanjundaswamy, K.; Goodenough, J. B. *J. Electrochem. Soc.* **1997**, *144*, 1188.
- (5) Yonemura, M.; Yamada, A.; Takei, Y.; Sonoyama, N.; Kanno, R. *J. Electrochem. Soc.* **2004**, *151*, A1352.

- (6) Delacourt, C.; Poizot, P.; Morcrette, M.; Tarascon, J.-M.; Masquelier, C. *Chem. Mater.* **2004**, *16*, 93–99.
- (7) Delacourt, C.; Laffont, L.; Bouchet, R.; Wurm, C.; Leriche, J.-B.; Morcrette, M.; Tarascon, J.-M.; Masquelier, C. *J. Electrochem. Soc.* **2005**, *152*, A913.
- (8) Kang, B.; Ceder, G. *J. Electrochem. Soc.* **2010**, *157*, A808.
- (9) Godshall, N. A.; Raistrick, I. D.; Huggins, R. A. *J. Electrochem. Soc.* **1984**, *131*, 543.
- (10) Hautier, G.; Jain, A.; Ong, S. P.; Kang, B.; Moore, C.; Doe, R.; Ceder, G. *Chem. Mater.* **2011**, *23*, 3945–3508.
- (11) Nanjundaswamy, K.; Padhi, A.; Goodenough, J. B.; Okada, S.; Otsuka, H.; Arai, H.; Yamaki, J. *Solid State Ionics* **1996**, *92*, 1–10.
- (12) Ceder, G.; Hautier, G.; Jain, A.; Ong, S. P. *MRS Bull.* **2011**, *36*, 185–191.
- (13) Meng, Y. S.; Arroyo-de Dompablo, M. E. *Energy Environ. Sci.* **2009**, *2*, 589.
- (14) Perdew, J.; Burke, K.; Ernzerhof, M. *Phys. Rev. Lett.* **1996**, *77*, 3865–3868.
- (15) Anisimov, V.; Zaanen, J.; Andersen, O. *Phys. Rev. B* **1991**, *44*, 943–954.
- (16) Anisimov, V. I.; Aryasetiawan, F.; Lichtenstein, A. I. *J. Phys: Condens. Matter* **1997**, *9*, 767–808.
- (17) Wang, L.; Maxisch, T.; Ceder, G. *Phys. Rev. B* **2006**, *73*, 195107.
- (18) Kubaschewski, O.; Alcock, C. B.; Spencer, P. J. *Thermochemical Data*. In *Materials Thermochemistry*, Sixth Edition; Pergamon Press: New York, 1993; Chapter 5, pp 257–323.
- (19) Mueller, T.; Hautier, G.; Jain, A.; Ceder, G. *Chem. Mater.* **2011**, *23*, 3854–3862.
- (20) Kresse, G.; Furthmüller, J. *Comput. Mater. Sci.* **1996**, *6*, 15–50.
- (21) Blöchl, P. *Phys. Rev. B* **1994**, *50*, 17953–17979.
- (22) Jain, A.; Hautier, G.; Moore, C. J.; Ong, S. P.; Fischer, C. C.; Mueller, T.; Persson, K. A.; Ceder, G. *Comput. Mater. Sci.* **2011**, *50*, 2295–2310.
- (23) Curtarolo, S.; Setyawan, W.; Wang, S.; Xue, J.; Yang, K.; Taylor, R. H.; Nelson, L. J.; Hart, G. L.; Sanvito, S.; Buongiorno-Nardelli, M.; Mingo, N.; Levy, O. *Comput. Mater. Sci.* **2012**, *58*, 227–235.
- (24) Ong, S. P.; Wang, L.; Kang, B.; Ceder, G. *Chem. Mater.* **2008**, *20*, 1798–1807.
- (25) Jain, A.; Hautier, G.; Ong, S. P.; Moore, C.; Fischer, C. C.; Ceder, G. *Phys. Rev. B* **2011**, *84*, 045115.
- (26) Aydinol, M.; Kohan, A.; Ceder, G.; Cho, K.; Joannopoulos, J. *Phys. Rev. B* **1997**, *56*, 1354–1365.
- (27) Hart, G. L. W.; Forcade, R. W. *Phys. Rev. B* **2008**, *77*, 224115.
- (28) Adams, S.; Rao, R. P. *Phys. Chem. Chem. Phys.* **2009**, *11*, 3210–3216.
- (29) Ong, S. P.; Jain, A.; Hautier, G.; Kang, B.; Ceder, G. *Electrochem. Commun.* **2010**, *12*, 427–430.
- (30) Chase, M. W. *NIST-JANAF Thermochemical Tables*; American Institute of Physics: Woodbury, NY, 1998.
- (31) Hautier, G.; Fischer, C. C.; Jain, A.; Mueller, T.; Ceder, G. *Chem. Mater.* **2010**, *22*, 3762–3767.
- (32) Nishimura, S.-i.; Nakamura, M.; Natsui, R.; Yamada, A. *J. Am. Chem. Soc.* **2010**, *132*, 13596–13597.
- (33) Zhou, H.; Upreti, S.; Chernova, N. A.; Hautier, G.; Ceder, G.; Whittingham, M. S. *Chem. Mater.* **2011**, *23*, 293–300.
- (34) Tamaru, M.; Barpanda, P.; Yamada, Y.; Nishimura, S.-i.; Yamada, A. *J. Mater. Chem.* **2012**, *22*, 24526–24529.
- (35) Ellis, B. L.; Makahnouk, W. R. M.; Makimura, Y.; Toghiani, K.; Nazar, L. F. *Nat. Mater.* **2007**, *6*, 749–753.
- (36) Wang, D.; Xiao, J.; Xu, W.; Nie, Z.; Wang, C.; Graff, G.; Zhang, J.-G. *J. Power Sources* **2011**, *196*, 2241–2245.
- (37) Hautier, G.; Ong, S. P.; Jain, A.; Moore, C. J.; Ceder, G. *Phys. Rev. B* **2012**, *85*, 155208.
- (38) Chen, H.; Hautier, G.; Jain, A.; Moore, C.; Kang, B.; Doe, R.; Wu, L.; Zhu, Y.; Tang, Y.; Ceder, G. *Chem. Mater.* **2012**, *24*, 2009–2016.
- (39) Chen, H.; Hautier, G.; Ceder, G. *J. Am. Chem. Soc.* **2012**, *134*, 19619–19627.

- (40) Patoux, S.; Wurm, C.; Morcrette, M.; Rouse, G.; Masquelier, C. *J. Power Sources* **2003**, *119–121*, 278–284.
- (41) Saïdi, M.; Barker, J.; Huang, H.; Swoyer, J. L.; Adamson, G. J. *J. Power Sources* **2003**, *119–121*, 266–272.
- (42) Yin, S.-C.; Grondey, H.; Strobel, P.; Anne, M.; Nazar, L. F. *J. Am. Chem. Soc.* **2003**, *125*, 10402–10411.
- (43) Makimura, Y.; Cahill, L. S.; Iriyama, Y.; Goward, G. R.; Nazar, L. F. *Chem. Mater.* **2008**, *20*, 4240–4248.
- (44) Jain, A.; Hautier, G.; Moore, C. J.; Kang, B.; Lee, J.; Chen, H.; Twu, N.; Ceder, G. *J. Electrochem. Soc.* **2012**, *159*, A622–A633.
- (45) Barker, J.; Saïdi, M. Y.; Swoyer, J. L. *J. Electrochem. Soc.* **2003**, *150*, A1394.
- (46) Barker, J.; Gover, R. K. B.; Burns, P.; Bryan, A. *Electrochem. Solid-State Lett.* **2005**, *8*, A285.
- (47) Ramesh, T. N.; Lee, K. T.; Ellis, B. L.; Nazar, L. F. *Electrochem. Solid-State Lett.* **2010**, *13*, A43.
- (48) Recham, N.; Chotard, J.-N.; Jumas, J.-C.; Laffont, L.; Armand, M.; Tarascon, J.-M. *Chem. Mater.* **2010**, *22*, 1142–1148.
- (49) Marx, N.; Croguennec, L.; Carlier, D.; Wattiaux, A.; Cras, F. L.; Suard, E.; Delmas, C. *Dalton Trans.* **2010**, *39*, 5108–5116.
- (50) Padhi, A.; Nanjundaswamy, K.; Masquelier, C.; Okada, S.; Goodenough, J. B. *J. Electrochem. Soc.* **1997**, *144*, 1609–1613.
- (51) Uebou, Y. *Solid State Ionics* **2002**, *148*, 323–328.
- (52) Barker, J.; Saïdi, Y.; Swoyer, J. *Alkali/transition metal halo- and hydroxy-phosphates and related electrode active materials*, U.S. Patent 6,964,827, 2005.
- (53) Barker, J.; Saïdi, M. Y.; Swoyer, J. *Lithium Metal Fluorophosphate and preparation thereof*, U.S. Patent 7,261,977, 2007.
- (54) Bhuvanewari, G. D.; Kalaiselvi, N. *Appl. Phys. A* **2009**, *96*, 489–493.
- (55) Aranda, M. A. G.; Bruque, S.; Attfield, J. P. *Angew. Chem., Int. Ed. (Engl. Transl.)* **1992**, *31*, 1090–1092.
- (56) Aranda, M.; Bruque, S.; Ramos-Barrado, J. *Solid State Ionics* **1993**, *65*, 407–410.
- (57) Aranda, M. *J. Solid State Chem.* **1997**, *132*, 202–212.
- (58) Ateba Mba, J.; Masquelier, C.; Suard, E.; Croguennec, L. *Chem. Mater.* **2012**, *24*, 1123–1234.
- (59) Shannon, R. D. *Acta Crystallogr., Sect. A: Cryst. Phys., Diffraction, Theor. Gen. Crystallogr.* **1976**, *32*, 751–767.
- (60) Hautier, G.; Fischer, C.; Ehrlacher, V.; Jain, A.; Ceder, G. *Inorg. Chem.* **2011**, *50*, 656–663.
- (61) Arroyo-de Dompablo, M. E.; Armand, M.; Tarascon, J. M.; Amador, U. *Electrochem. Commun.* **2006**, *8*, 1292–1298.
- (62) Arroyo y de Dompablo, M.; Amador, U.; Tarascon, J.-M. *J. Power Sources* **2007**, *174*, 1251–1257.
- (63) Ellis, B. L.; Nazar, L. F. *Chem. Mater.* **2012**, *24*, 966–968.
- (64) Chevrier, V. L.; Ong, S. P.; Armiento, R.; Chan, M. K. Y.; Ceder, G. *Phys. Rev. B* **2010**, *82*, 075122.
- (65) Heyd, J.; Scuseria, G. E.; Ernzerhof, M. *J. Chem. Phys.* **2003**, *118*, 8207.